Supporting Information

Single Molecule Magnet Behaviour Enhanced by Synergic Effect of Single-ion Anisotropy and Magnetic Interactions

Li Zhang,[‡] Yi-Quan Zhang,[*,†] Peng Zhang,[*,§] Lang Zhao,[‡] Mei Guo,[‡] Jinkui Tang[*,‡]

[†]Jiangsu Key Laboratory for NSLSCS, School of Physical Science and Technology, Nanjing Normal University, Nanjing 210023, P. R. China

[‡]State Key Laboratory of Rare Earth Resource Utilization, Changchun Institute of Applied Chemistry, Chinese Academy of Sciences, Changchun 130022, P. R. China

[§]Institut für Physikalische Chemie, Universität Stuttgart, Pfaffenwaldring 55, D-70569, Stuttgart, Germany

Experimental Section

Materials and Physical Measurements. All reagents and solvents were obtained from commercial sources and were used without further purification. Elemental analyses (EA) for C, H, and N were performed with a Perkin-Elmer 2400 analyzer. FTIR spectra (Figure S1) were recorded with a Nicolet 6700 IR Fourier spectrometer equipped with a smart ATR FTIR attachment in the range of 4000-500 cm^{-1}. Magnetic data were carried out on a Quantum Design MPMS-XL7 SQUID magnetometer equipped with a 7 T magnet. The direct current (dc) measurements were collected with an external magnetic field of 1000 Oe in the temperature range 1.9-300 K, and the alternating-current (ac) measurements were measured in a 3.0 Oe ac field oscillating at different frequencies from 0.05 to 1500 Hz. The experimental magnetic susceptibility data are corrected for the diamagnetism estimated from Pascal's tables[1] and sample holder calibration.

Crystallographic data collection and refinement. Crystallographic data of complexes **1-3** were collected on a Bruker Apex II charge-coupled device (CCD) diffractometer with graphite monochromated Mo-Kα radiation (λ = 0.71073 Å) at 186 (2) K. The structures were solved by direct methods and refined on F^2 by full-matrix least squares by means of SHELXS-97 and SHELXL-97 programs[2]. The location of Dy atoms was easily determined, and O, N and C atoms were subsequently determined from the difference Fourier maps. All non-hydrogen atoms were refined with anisotropic thermal parameters. The H atoms were introduced in calculated positions and refined with fixed geometry with respect to their carrier atoms. CCDC-1507443 (**1**), 1507444 (**2**), 1507447 (**2a**), 1507445 (**3**), and 1507446 (**3a**) contain the supplementary crystallographic data for this paper. These data can be obtained free of charge from the Cambridge Crystallographic Data Centre via www.ccdc.cam.ac.uk/data_request/cif.

Synthesis of Ligand: The hydrazone ligand H$_3$L (3-hydroxy-N'-(2-hydroxy-3-methoxybenzylidene) picolinohydrazide) was synthesized according to the reported procedure[3]. Yield: 85%. Elemental analysis (%) calcd for C$_{14}$H$_{13}$N$_3$O$_4$:C, 58.53, H, 4.56, N, 14.63; found: C, 58.90, H, 4.58, N, 14.52.IR (KBr, cm^{-1}): 3140 (w), 2963 (br), 2831 (w), 1650 (m), 1606 (s), 1579 (m), 1538 (s), 1460 (s), 1442 (s), 1389 (w), 1330 (m), 1303 (s), 1246 (s), 1229 (s), 1197 (s), 1147 (w), 1118 (m), 1081 (m), 971 (w), 909 (m), 824 (w), 805 (m), 770 (m), 729 (s), 690 (m), 670 (m), 576 (w).
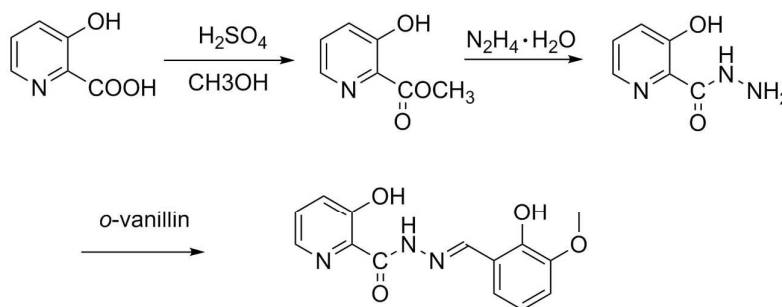
Synthesis of [Dy$_2$(HL)$_2$(NO$_3$)$_2$(CH$_3$CN)$_2$]·2CH$_3$CN (1). A mixture of Dy(NO$_3$)$_3$·6H$_2$O (0.1 mmol, 0.046 g) and H$_3$L (0.1 mmol, 0.029 g) in CH$_3$OH / CH$_3$CN (5 mL / 10 mL) was treated with Et$_3$N (0.1 mmol, 0.014 mL). The resultant yellow solution was stirred for 4 h and then was exposed to air to allow the slow evaporation of the solvent. Yellow blocks of **1** suitable for X-ray diffraction analysis were collected after one week. Yield: 22 mg (37%, based on Dy). Elemental analysis (%) calcd for C$_{36}$H$_{34}$Dy$_2$N$_{12}$O$_{14}$: C, 36.53, H, 2.90, N, 14.20; found: C, 36.76, H, 2.87 N, 14.31. IR (cm^{-1}): 3613 (w), 3394 (br), 3001 (br), 1597 (s), 1556 (m), 1512 (m), 1467 (m), 1447 (s), 1341 (w), 1310 (m), 1273 (m), 1257 (m), 1248 (m), 1220 (s), 1170 (w), 1148 (w), 1118 (w), 1079 (w), 1022 (w), 972 (w), 929 (w), 858 (w), 810 (w), 778 (w), 741 (m), 687 (w), 639 (w), 568 (w), 550 (w).

Synthesis of [Dy$_2$(HL)$_2$(NO$_3$)$_2$(DMF)$_2$]·2H$_2$O (2). A mixture of Dy(NO$_3$)$_3$·6H$_2$O (0.1 mmol, 0.046 g) and H$_3$L (0.1 mmol, 0.029 g) in CH$_3$OH / CH$_3$CN (14 mL / 7 mL) was treated with LiOH·H$_2$O (0.1 mmol, 0.004 g) and the resultant yellow solution was stirred for 4 h. Yellow needles of **2** were obtained by diffusing diethyl ether slowly into the solution after two weeks. Yield: 20 mg (33%, based on Dy). Elemental analysis (%) calcd for C$_{34}$H$_{40}$Dy$_2$N$_{10}$O$_{18}$: C, 33.98, H, 3.35, N, 11.66; found: C, 34.92, H, 3.39, N, 11.95. IR (cm^{-1}): 3613 (w), 3400 (br), 2927 (br), 1662 (s), 1600 (s), 1554 (m), 1504 (s), 1466 (s), 1447 (s), 1380 (m), 1337 (m), 1308 (m), 1273 (s), 1243 (s), 1220 (s), 1172 (w), 1150 (w), 1117 (m), 1079 (w), 1021 (m), 966 (w), 928 (w), 859 (w), 811 (w), 744 (m), 682 (m), 639 (w), 568 (w), 546 (w).

Synthesis of {[Y$_2$(HL)$_2$(NO$_3$)$_2$(DMF)$_2$]·CH$_3$CN}$_2$ (2a). The procedure was the same as that used for complex **2** except that Y(NO$_3$)$_3$·6H$_2$O (0.1 mmol, 0.038 g) replaced Dy(NO$_3$)$_3$·6H$_2$O. Yellow needles of **2a** were obtained after two weeks. Yield: 23 mg (43%, based on Y).

Synthesis of Dilution Sample 2@Y. The procedure was the same as that used for the pure **2** except that accurately measured 19:1 molar ratios of the yttrium(III) and dysprosium(III) nitrate was used as rare-earth salt instead of dysprosium(III) nitrate.

Synthesis of Dy$_2$(HL)$_2$(NO$_3$)$_2$(DMF)$_4$ (3). A mixture of Dy(NO$_3$)$_3$·6H$_2$O (0.1 mmol, 0.046 g) and H$_3$L (0.1 mmol, 0.029 g) in CH$_3$OH / CH$_3$CN (5 mL / 10 mL) was treated with Et$_3$N (0.2 mmol, 0.028 mL). The yellow solution was stirred for 4 h and subsequently filtered. The resulting yellow precipitation was dried and redissolved in DMF (15 mL). Then diethyl ether was allowed to diffuse slowly into the solution at room temperature and yellow blocks of **3** were collected after one month. Yield: 16 mg (24%, based on Dy). Elemental analysis (%) calcd for C$_{40}$H$_{50}$Dy$_2$N$_{12}$O$_{18}$: C, 36.62, H, 3.84, N, 12.81; found: C, 36.77, H, 3.85, N, 12.74. IR (cm^{-1}): 2935 (br), 1662 (s), 1602 (s), 1552 (m), 1503 (m), 1467 (s), 1448 (s), 1380 (m), 1340 (m), 1305 (m), 1250 (m), 1238 (m), 1220 (s), 1150 (w), 1110 (m), 1077 (w), 1025 (w), 968 (w), 927 (w), 862 (w), 812 (w), 768 (w), 739 (m), 700 (w), 685 (m), 665 (w), 637 (w), 567 (w), 547 (w).

Synthesis of Y$_2$(HL)$_2$(NO$_3$)$_2$(DMF)$_4$ (3a). The procedure was the same as that used for complex **3** except that Y(NO$_3$)$_3$·6H$_2$O (0.1 mmol, 0.038 g) replaced Dy(NO$_3$)$_3$·6H$_2$O. Yellow blocks of **3a** were obtained after three weeks. Yield: 15 mg (26%, based on Y).

Synthesis of Diluted Sample 3@Y. The procedure was the same as that used for the pure **3** except that accurately measured 19:1 molar ratios of the yttrium(III) and dysprosium(III) nitrate was used as rare-earth salt instead of dysprosium(III) nitrate.
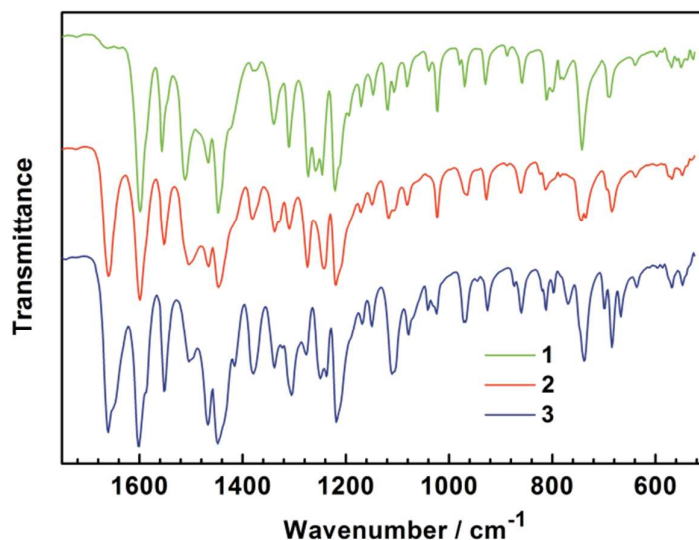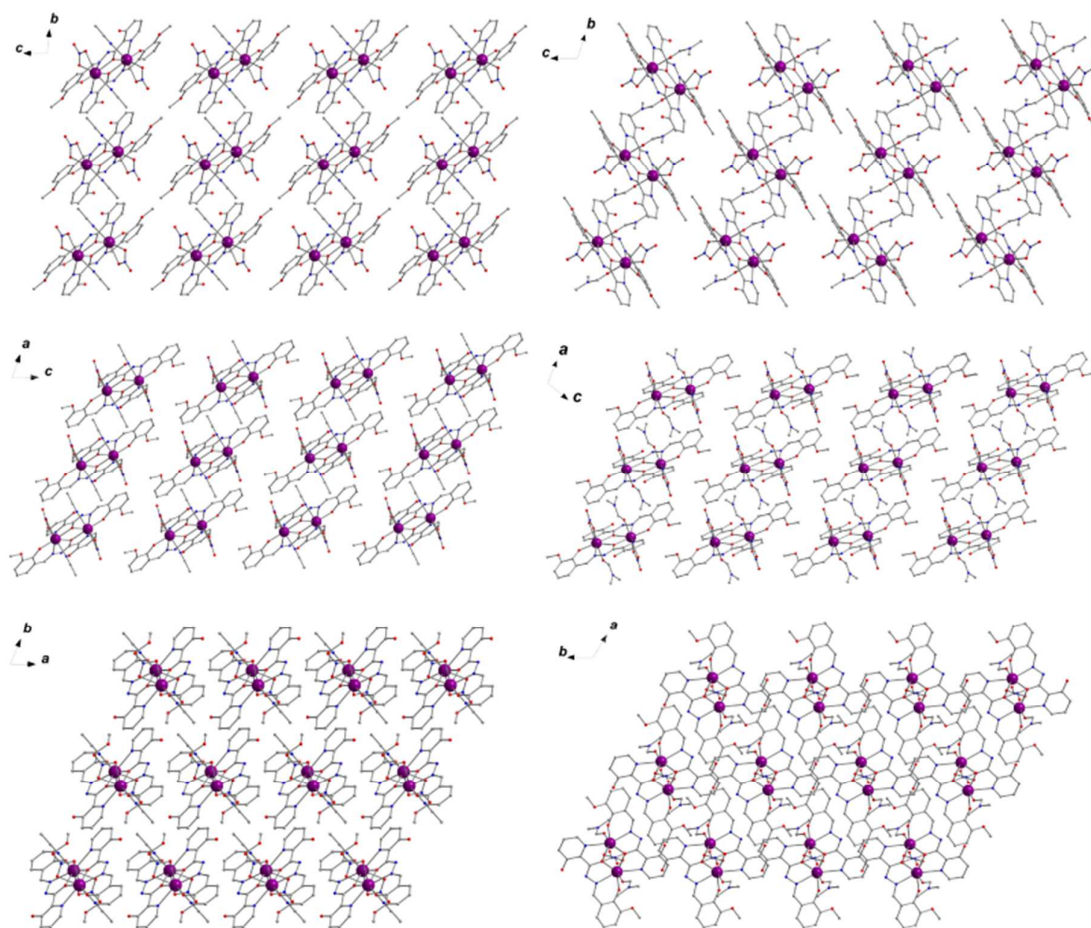

Figure S1. Infrared spectra of **1-3**.

Figure S2. Packing arrangement along the crystallographic *a*, *b* and *c*axis for complexes**1** (left) and **2** (right).Color code: purple, Dy; red, O; blue, N; gray, C.
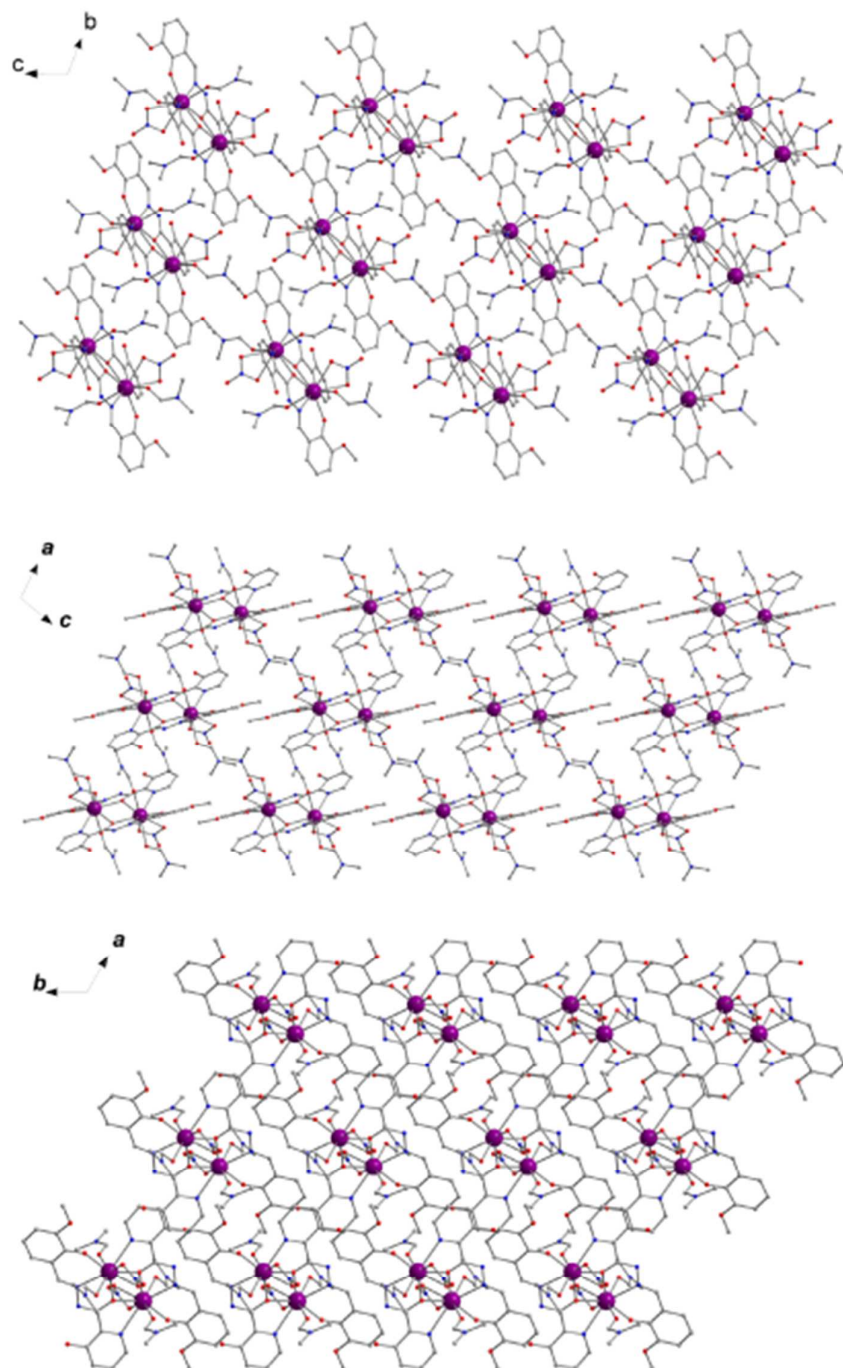
Figure S3. Packing arrangements along the crystallographic *a*, *b* and *c* axis for complex **3**. Color code: purple, Dy; red, O; blue, N; gray, C.
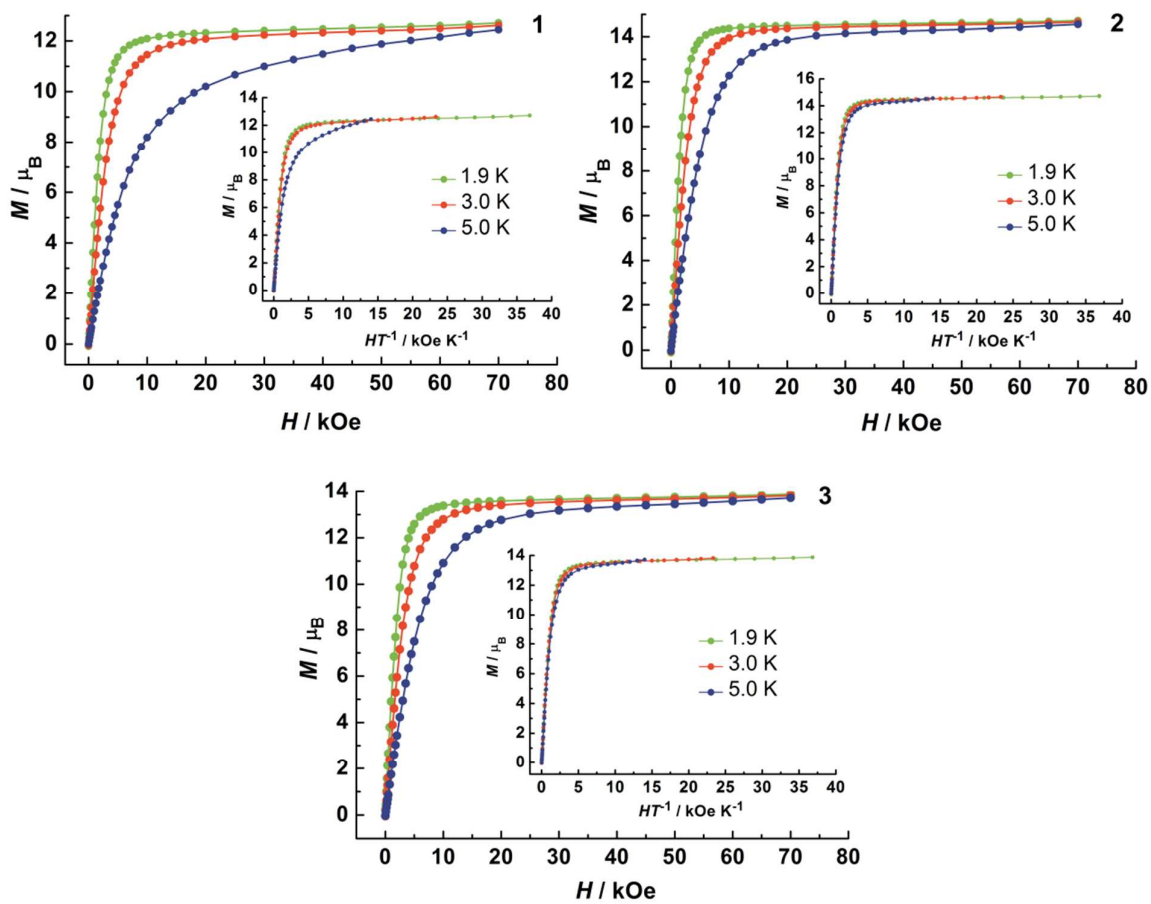
Figure S4. Field dependences of magnetization in the field range 0-70 kOe and at the range of 1.9-5.0 K. Insets: Plots of the reduced magnetization M versus H/T for **1-3**.
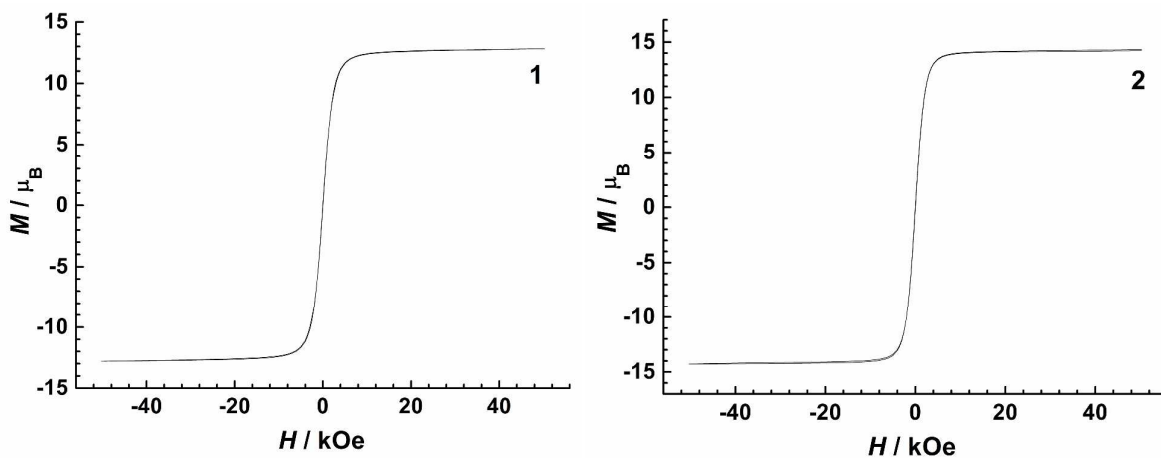
Figure S6. Frequency dependence of in-phase ac susceptibilities under zero dc field over the temperature range of 1.9-5 K for **1**. Inset: Corresponding frequency dependence of the out-of-phase ac susceptibility.

Figure S7. Frequency dependence of in-phase ac susceptibilities under zero dc field over the temperature range of 1.9-4.5 K for **2**. Inset: Corresponding frequency dependence of the out-of-phase ac susceptibility.
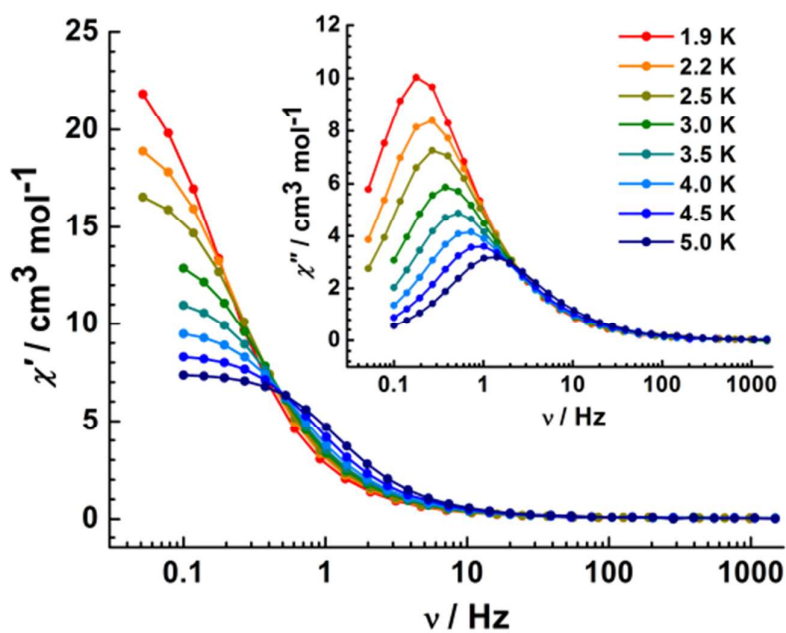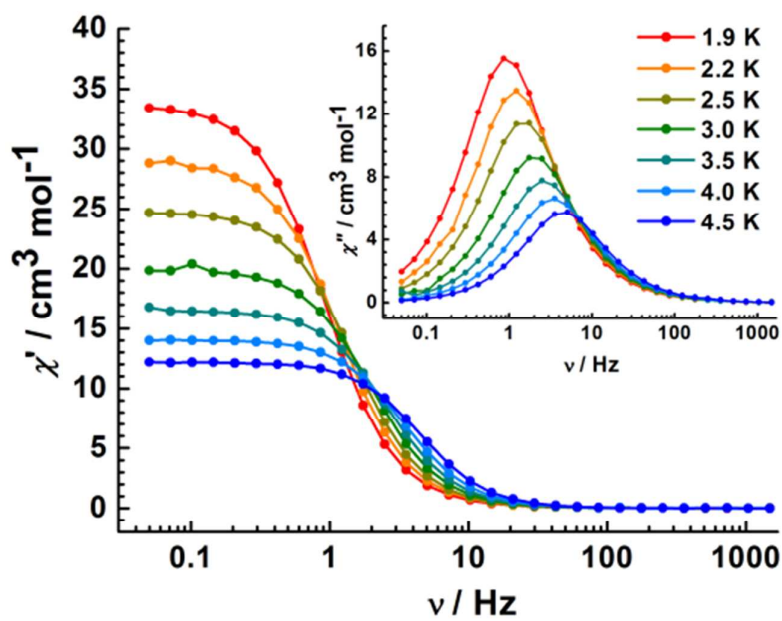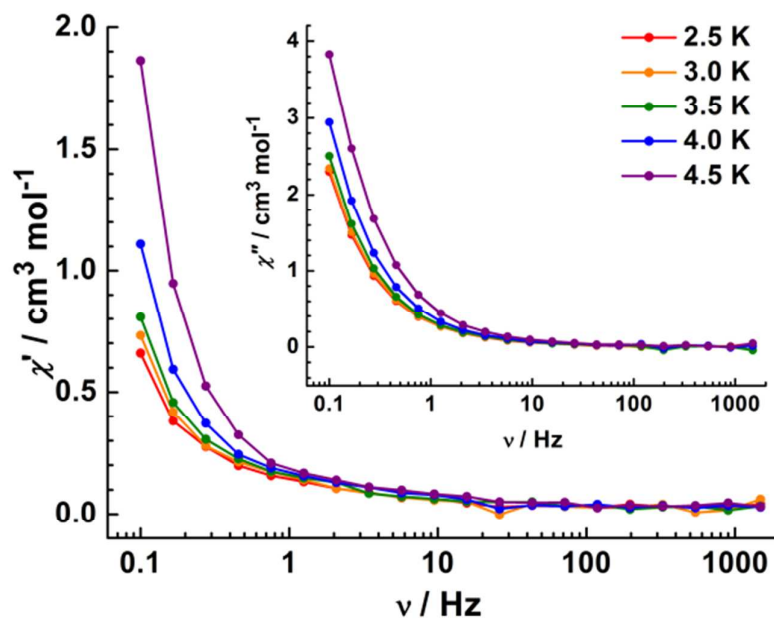
Figure S8. Frequency dependence of in-phase ac susceptibilities under zero dc field over the temperature range of 2.5-4.5 K for **3**. Inset: Corresponding frequency dependence of the out-of-phase ac susceptibility.
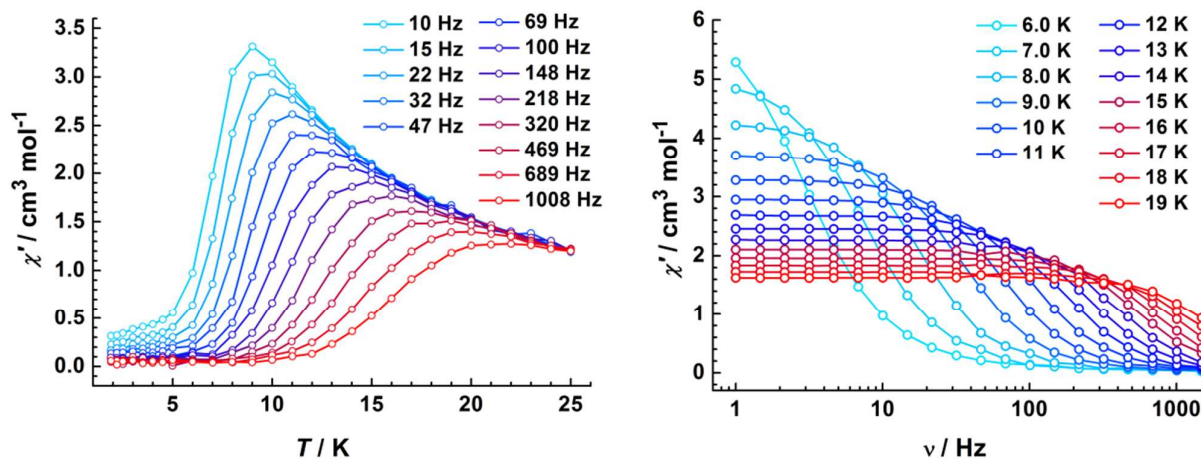

Figure S9. Temperature (left) and frequency(right) dependence of the in-phase ac susceptibility under zero dc field for **1**.
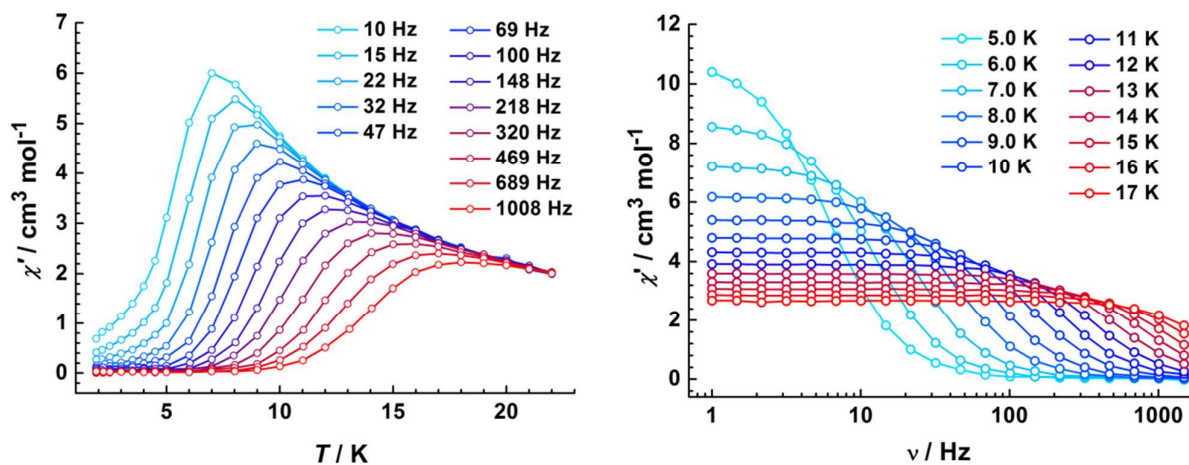
Figure S10. Temperature (left) and frequency(right) dependence of the in-phase ac susceptibility under zero dc field for **2**.
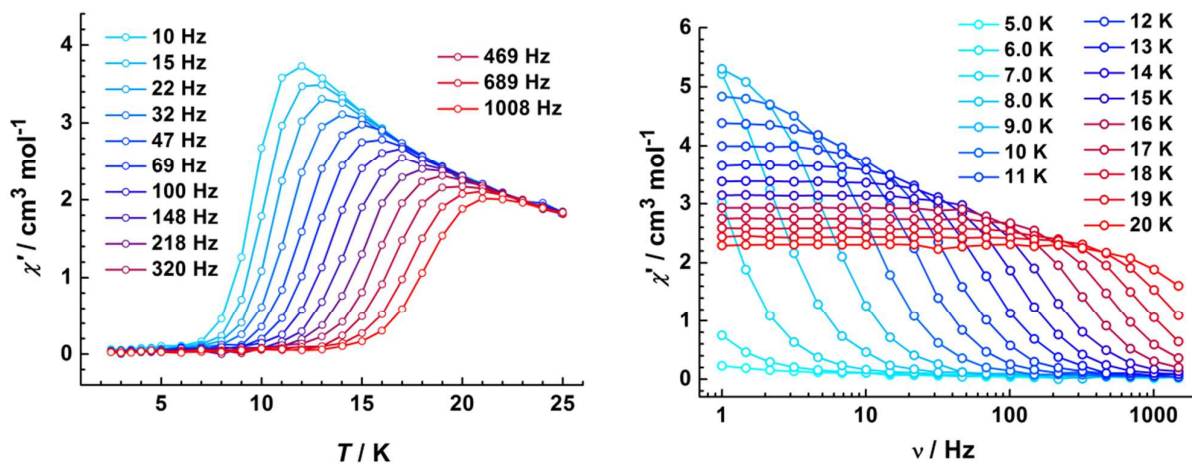
Figure S11. Temperature (left) and frequency (right) dependence of the in-phase ac susceptibility under zero dc field for **3**.
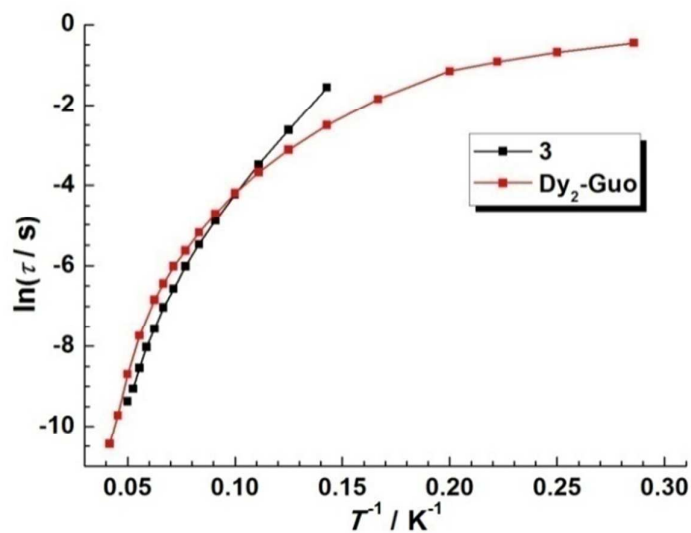
Figure S12. Magnetization relaxation time, $\ln\tau$ versus T^{-1} for **3** and Dy_2 reported by Guo et al[4] under zero dc field. The solid lines are guides for the eyes.
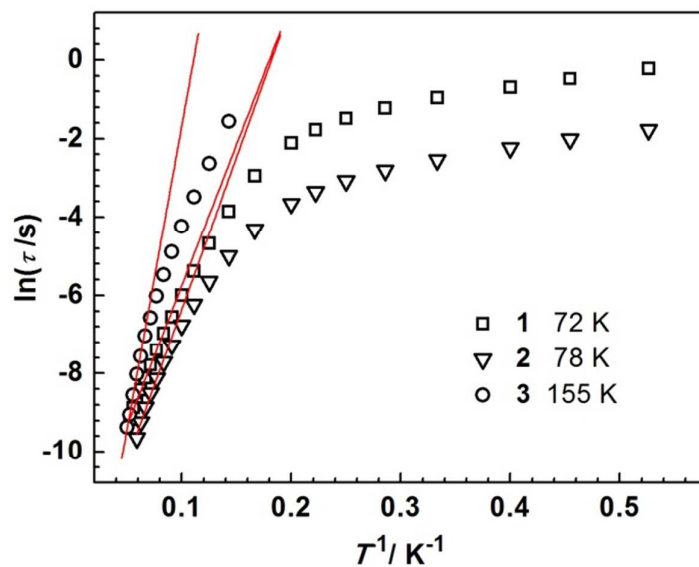
Figure S13. Magnetization relaxation time, $\ln\tau$ versus T^{-1} for **1-3** under zero dc field. The solid lines correspond to the best fit of the experimental data to the Arrhenius law.
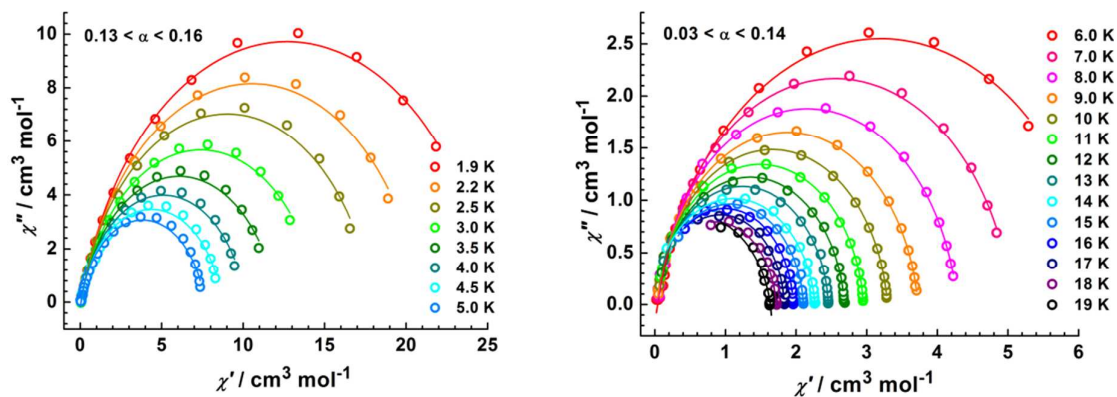
Figure S14. The Cole-Cole diagrams for **1** at different temperatures under zero dc field. The solid lines represent the best fit obtained with a generalized Debye model.
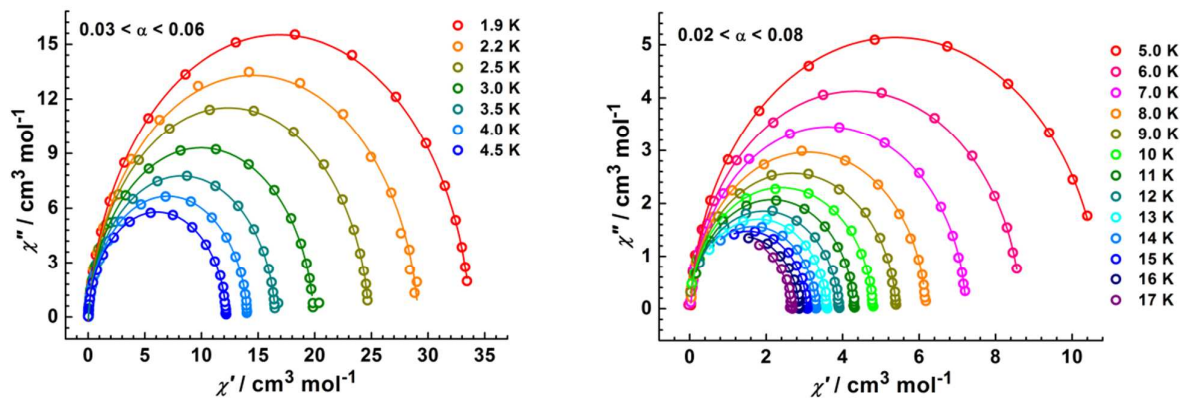
Figure S15. The Cole-Cole diagrams for **2** at different temperatures under zero dc field. The solid lines represent the best fit obtained with a generalized Debye model.
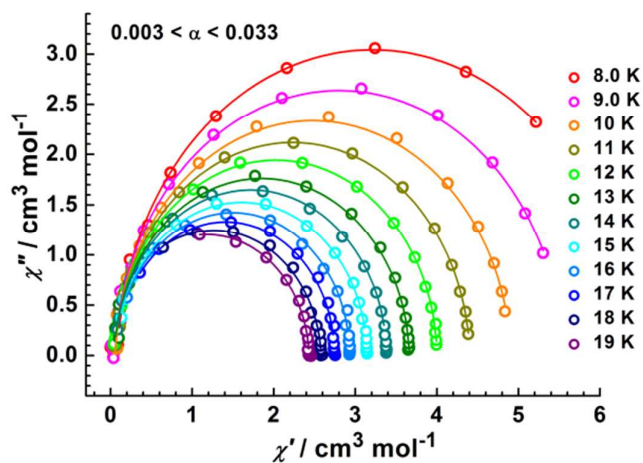
Figure S16. The Cole-Cole diagrams for **3** at different temperatures under zero dc field. The solid lines represent the best fit obtained with a generalized Debye model.
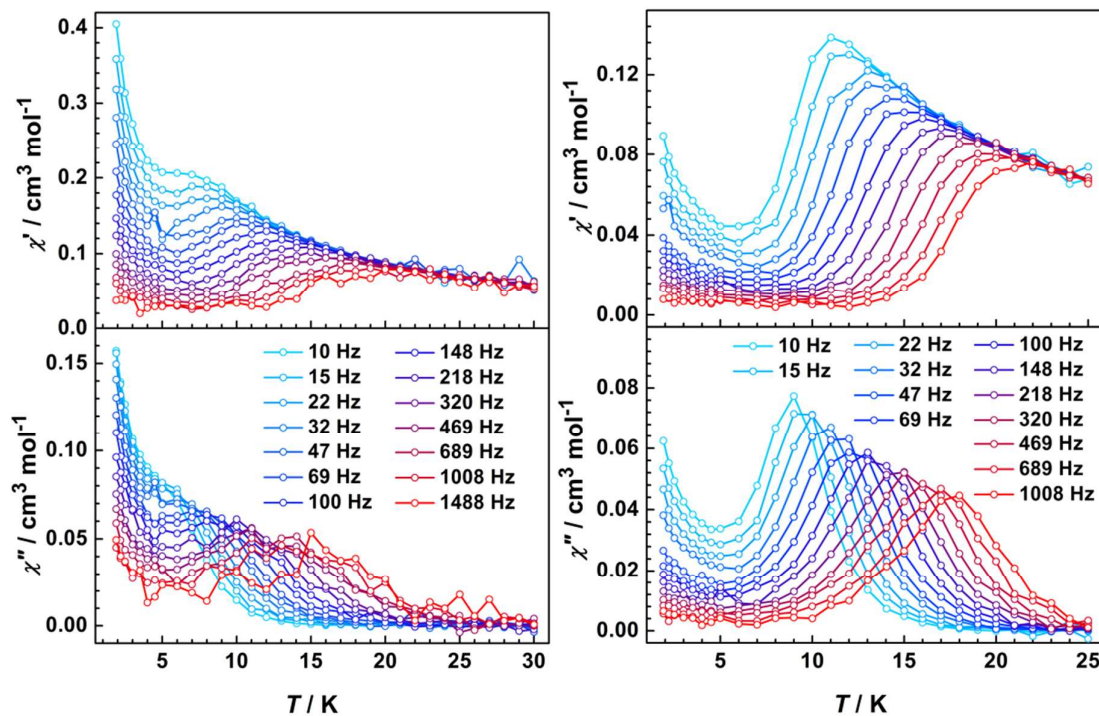
Figure S17. Temperature dependence of the ac magnetic susceptibility under zero dc field for **2**@Y (left) and **3**@Y (right).
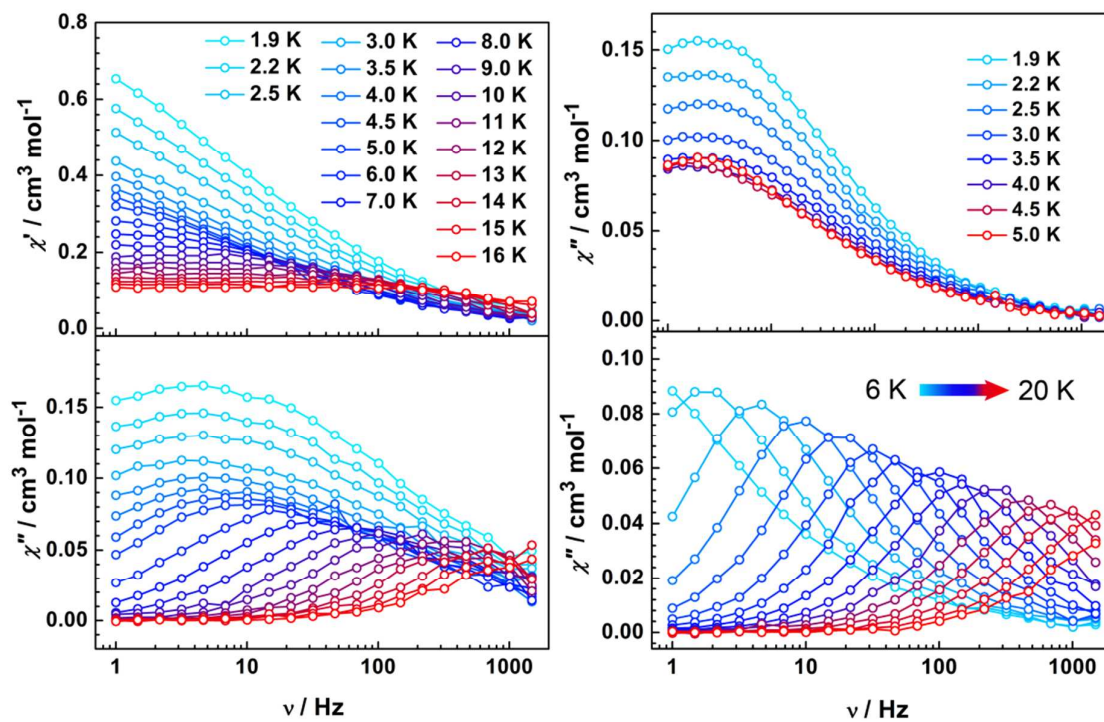
Figure S18. Frequency dependence of the ac magnetic susceptibility under zero dc field for **2**@Y (left) and **3**@Y (right).
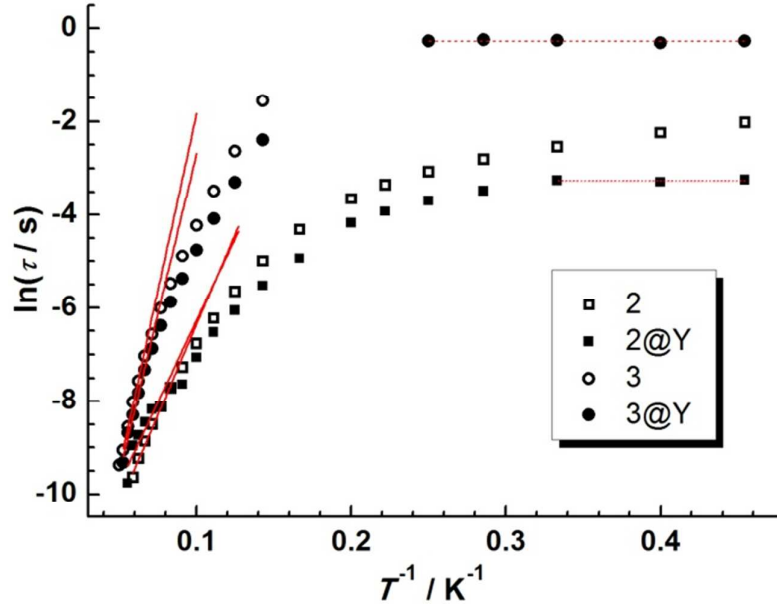
Figure S19. Magnetization relaxation time, lnτ versus T^{-1} for **2** and **3** together with their diluted samples under zero dc field. The solid lines correspond to the best fit of the experimental data to the Arrhenius law.
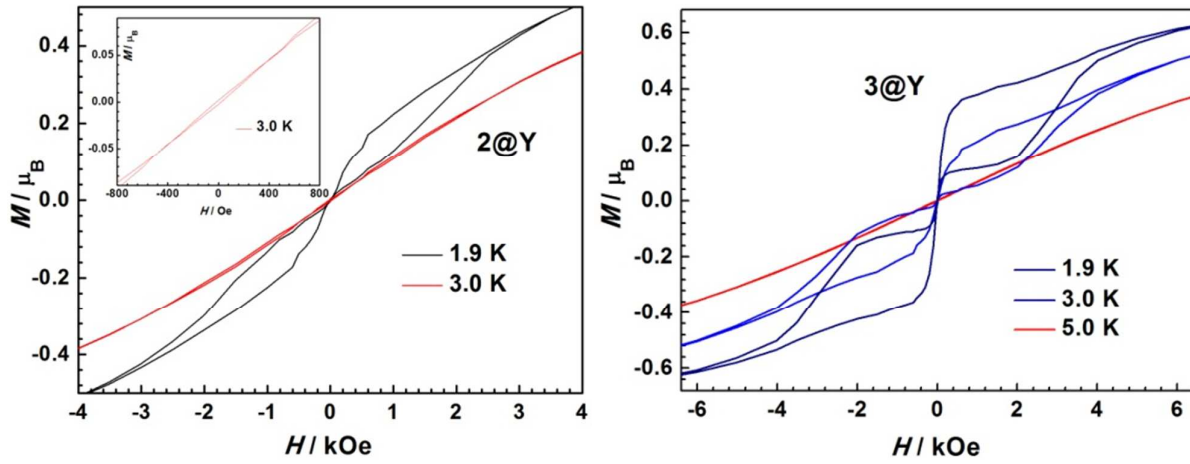

Figure S20. Plots of magnetization M versus field H for **2**@Y (left) and **3**@Y (right).
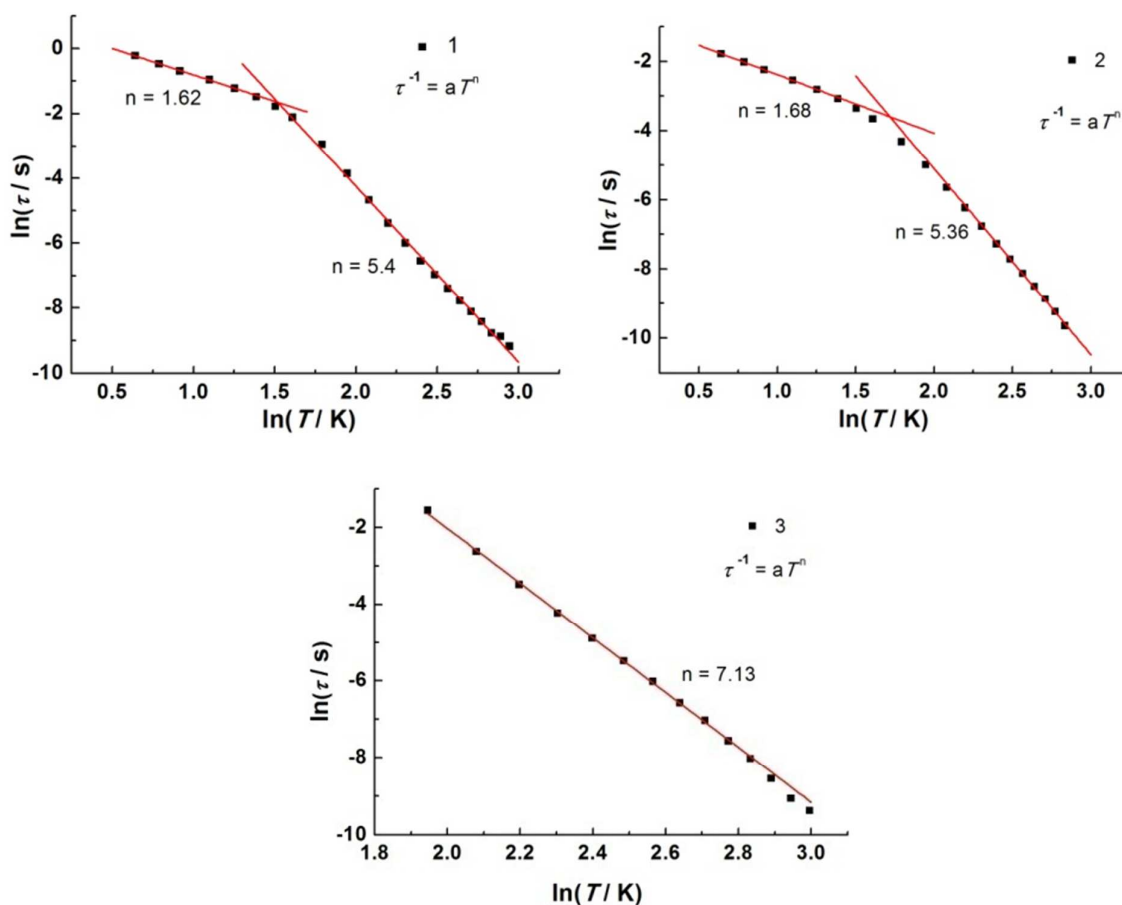
Figure S21. The relaxation time as a function of the temperature can be fitted to Raman process for compounds **1-3**.

Ab initio Calculations for 1-3

Complete-active-space self-consistent field (CASSCF) calculations on individual lanthanide Dy^{III} fragments of complexes **1-3** on the basis of X-ray determined geometry have been carried out with MOLCAS 7.8 program package.[5] During the calculations, the other Dy^{III} ion was replaced by diamagnetic Lu^{III}. The basis sets for all atoms are atomic natural orbitals from the MOLCAS ANO-RCC library: ANO-RCC-VTZP for Dy^{III} ions; VTZ for close O and N; VDZ for distant atoms. The calculations employed the second order Douglas-Kroll-Hess Hamiltonian, where scalar relativistic contractions were taken into account in the basis set and the spin-orbit couplings were handled separately in the restricted active space state interaction (RASSI-SO) procedure. For the fragment of Dy^{III}, active electronsin 7 active spaces include all f electrons (CAS(9 in 7) in the CASSCF calculation. We have mixed the maximum number of spin-free state which was possible with our hardware (all from 21 sextets, 128 from 224 quadruplets, 130 from 490 doublets for the Dy^{III} fragment).
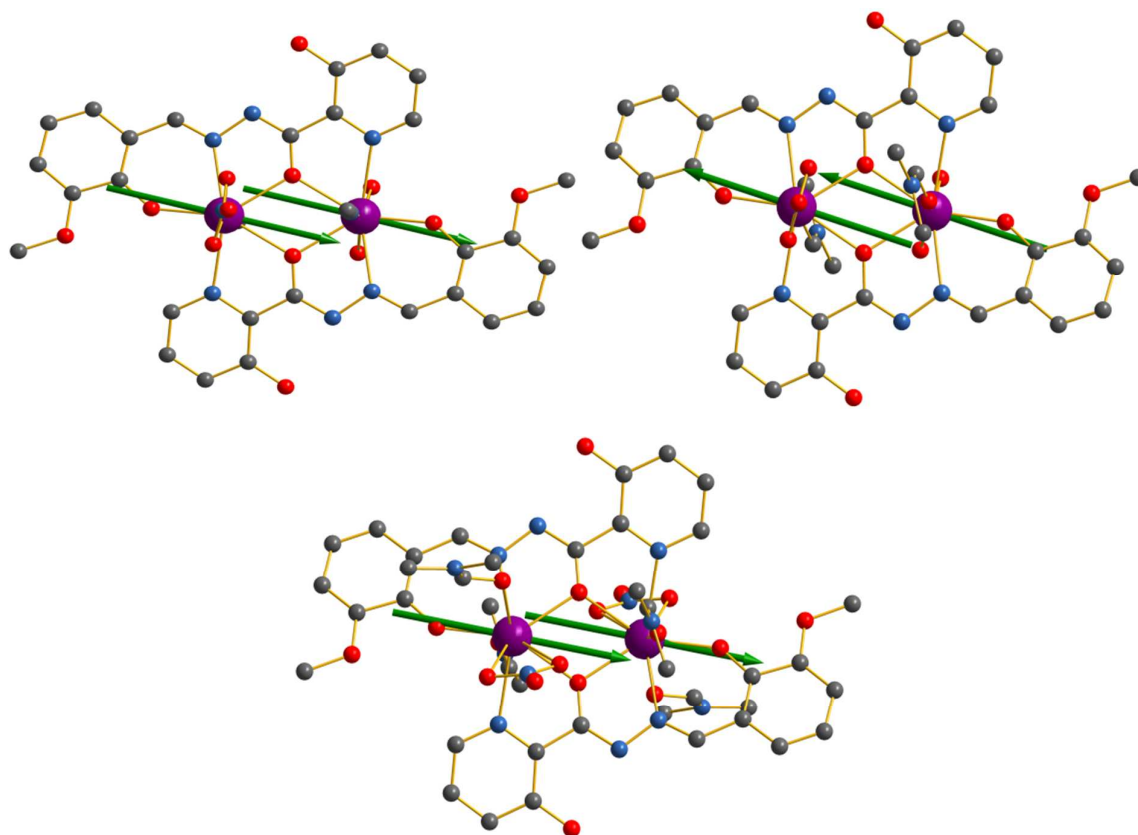
Figure S22. Orientations of the local main magnetic axes of the ground doublets on Dy^{III} ions for compounds **1-3**.

Fitting the exchange interaction in four complexes using Lines model based on CASSCF results

To fit the exchange interactions in four complexes, we took two steps to obtain them. Firstly, we calculated the mononuclear fragments using CASSCF to obtain the corresponding magnetic properties (see the first part). And then, the exchange interaction between the magnetic centers is considered within the Lines model,[6] while the account of the dipole-dipole magnetic coupling is treated exactly.

For complexes **1-3**, the exchange Hamiltonian is:

$$\hat{H}_{exch} = -J_{Dy-Dy}^{total} \, \hat{\tilde{S}}_{Dy1} \, \hat{\tilde{S}}_{Dy2} \tag{1}$$

The J_{Dy-Dy}^{total} is parameter of the total magnetic interaction ($J^{total} = J^{diploar} + J^{exchange}$) between magnetic center ions. The $\hat{\tilde{S}}_{Dy} = \pm 1/2$ is the ground pseudospin on the Dy site. The dipolar magnetic coupling can be calculated exactly, while the exchange coupling constants were fitted through comparison of the computed and measured magnetic susceptibility and molar magnetization using the

POLY_ANISO program.[7] The intermolecular interaction zJ' of **1-3** were all set to -0.01 cm^{-1}.

Table S1. Crystallographic data and structure refinement details for compounds.

Compound	**1**	**2**	**2a**	**3**	**3a**
Formula	$C_{36}H_{34}Dy_2N_{12}O_{14}$	$C_{34}H_{40}Dy_2N_{10}O_{18}$	$C_{72}H_{78}N_{22}O_{32}Y_4$	$C_{40}H_{50}Dy_2N_{12}O_{18}$	$C_{40}H_{50}N_{12}O_{18}Y_2$
Mr	1183.75	1201.76	2119.20	1311.92	1164.74
Crystal system	Triclinic	Triclinic	triclinic	Triclinic	Triclinic
Space group	P-1	P-1	P-1	P-1	P-1
T [K]	186(2)	186(2)	186(2)	186(2)	186(2)
a [Å]	9.578(4)	10.2501(11)	9.5958(13)	10.2781(15)	10.2368(5)
b [Å]	10.065(4)	10.5255(12)	11.5682(17)	10.5714(15)	10.4594(5)
c [Å]	13.001(5)	13.2560(15)	20.537(3)	13.439(2)	13.2859(6)
α [°]	87.307(7)	100.689(2)	104.335(3)	105.061(3)	104.7200(10)
β [°]	69.549(6)	100.032(2)	93.618(3)	94.880(3)	95.0630(10)
γ [°]	68.064(7)	118.179(2)	95.026(3)	116.840(3)	116.5670(10)
V [Å^3]	1084.2(7)	1180.8(2)	2191.8(5)	1222.9(3)	1196.59(10)
Z	1	1	1	1	1
ρ_{calcd} [g cm^{-3}]	1.813	1.690	1.606	1.781	1.616
μ(Mo-Kα) [mm^{-1}]	3.498	3.218	2.717	3.116	2.500
F (000)	578	590	1076	650	596
Reflns collected	6907	7538	7412	7852	7539
Unique reflns	4315	4684	4236	4876	4724
R_{int}	0.0206	0.0184	0.0576	0.1238	0.0225
Param/restraints	293 / 0	302 / 0	595 / 12	331 / 0	331 / 0
GOF	1.060	1.096	1.075	1.132	1.087
R_1 [I > 2σ(I)]	0.0293	0.0272	0.0871	0.0669	0.0332
wR_2 (all data)	0.0739	0.0835	0.2674	0.1655	0.0900

Table S2. Natural Bond Order (NBO) charges per atoms in the ground state of complexes **1-3** calculated within CASSCF (see Figure. 1).

	1	2	3
Dy1	2.509	2.526	2.519
O1	−0.768	−0.774	−0.762
O1*	−0.764	−0.775	−0.731
O2	−0.899	−0.884	−0.860
O8			−0.709
O9			−0.689
N1*	−0.340	−0.336	−0.323
N2	−0.349		
N3	−0.327	−0.336	−0.294

	1	2	3
$\chi_M T$ expected value at rt (cm^3 K mol^{-1})	28.34	28.34	28.34
$\chi_M T$ experimental value at rt (cm^{3}Kmol^{-1})	27.48	26.90	29.50
$\chi_M T$ experimental minimum value (cm^{3}Kmol^{-1})	25.09	25.40	29.48
$\chi_M T$ experimental value at 2.0 K (cm^{3}Kmol^{-1})	35.12	36.25	41.63

Table S4. Lowest Kramers doublets (cm^{-1}) and the **g** (g_x, g_y, g_z) tensors on individual Dy^{III} fragments of **1-3**.

1		2		3	
Dy^{III}		Dy^{III}		Dy^{III}	
E	**g** ($\tilde{s}=1/2$)	E	**g** ($\tilde{s}=1/2$)	E	**g** ($\tilde{s}=1/2$)
0.00	0.0033	0.00	0.0071	0.00	0.0001
	0.0062		0.0139		0.0024
	19.6665		19.6121		19.6859
213.11	0.0995	203.84	0.0774	139.49	0.0495
	0.1199		0.0963		0.0665
	17.0032		16.9938		17.2874
405.86	9.8031	390.23	2.6735	257.20	1.1077
	7.4852		4.9081		1.1838
	2.1582		10.8130		13.8369
440.38	1.8791	434.45	1.1949	299.78	2.4207
	4.3411		5.4395		4.9990
	11.7039		10.4198		13.5086
533.80	5.0524	457.74	0.6725	335.22	1.7060

	6.7035		3.3879		5.2929
	8.5665		13.0599		11.1875
605.84	0.3838	523.48	3.4016	378.23	1.8155
	1.0403		3.8697		2.5685
	18.6030		11.6299		12.8854
624.44	0.1661	569.75	0.5040	425.67	1.1287
	0.6785		3.1994		1.5271
	14.2891		12.5156		13.4308
699.36	0.4490	603.49	1.3869	467.94	0.0352
	0.8348		3.8320		0.2145
	18.0984		15.2776		16.6752

Table S5. Parameters obtained from fitting temperature-dependent relaxation times τ.

	A (s^{-1} K^{-1})	B (s^{-1} K^{-1})	N	τ_{QTM} (s)	τ_0(s)
1	0.669	$8.09*10^{-4}$	5.61	-	-
2	3.47	0.00421	5.30	-	-
2@Y	0	0.0532	4.28	0.0444	-
3	0	$6.39*10^{-6}$	7.00	-	$1.21*10^{-8}$
3@Y	0	$3.54*10^{-5}$	6.48	0.797	$9.02*10^{-9}$

References

(1) Boudreaux, E. A.; Mulay, L. N. Theory and Applications of Molecular Paramagnetism, John Wiley & Sons, New York, 1976.

(2) (a) Tian, H.; Guo, Y.-N.; Zhao, L.; Tang, J.; Liu, Z. *Inorg. Chem.*, **2011**, *50*, 8688; (b) Zhang, L.; Zhang, P.; Zhao, L.; Wu, J.; Guo, M.; Tang, J. *Inorg. Chem.*, **2015**, *54*, 5571.

(3) (a) Sheldrick, G. M. SHELXS-97, Program for Crystal Structure Solution, University of Göttingen, Germany, 1997; (b) Sheldrick, G. M. SHELXL-97, Program for Crystal Structure Refinement, University of Göttingen, Germany, 1997.

(4) Guo, Y.-N.; Xu, G.-F.; Wernsdorfer, W.; Ungur, L.; Guo, Y.; Tang, J.; Zhang, H.-J.; Chibotaru, L. F.; Powell, A. K. *J. Am. Chem. Soc.*, **2011**, *133*, 11948.

(5) Karlström, G.; Lindh, R.; Malmqvist, P.-Å.; Roos, B. O.; Ryde, U.; Veryazov, V.; Widmark, P.-O.; Cossi, M.; Schimmelpfennig, B.; Neogrady, P.; Seijo, L. MOLCAS: a Program Package for Computational Chemistry. *Comput. Mater. Sci.* **2003**, *28*, 222.

(6) Lines, M. E. *J. Chem. Phys*. **1971**, *55*, 2977.

(7) (a) Chibotaru, L. F.; Ungur, L.; Soncini, A. *Angew. Chem. Int. Ed.*, **2008**, *47*, 4126; (b) Ungur, L.; Van den Heuvel, W.; Chibotaru, L.F. *New J. Chem.*, **2009**, *33*, 1224; (c) Chibotaru, L. F.; Ungur, L.; Aronica,C.; Elmoll, H.; Pilet, G.; Luneau, D. *J. Am. Chem. Soc.*, **2008**, *130*, 12445.